ICANS XIV
14th Meeting of the International Collaboration on Advanced Neutron Sources,
Starved Rock Lodge, Utica, Ill, USA
June 14-19, 1998

Heat Transfer and Thermomechanic Analyses on the Test Rods in the SINQ-Target Mark 2

L. Ni and G S. Bauer
Paul Scherrer Institute, CH-5232 Villigen-PSI, Switzerland

Abstract

The thermal and mechanical loads anticipated on the experimental target elements filled with test samples (Zircaloy cladding) or Lead (steel cladding) of the SINQ target Mark 2 were examined by means of a coupled thermomechanical analysis. It could be shown that in no case stress levels are to be expected on the cladding that would be near the engineering limits of the materials in question, in particular if the plasticity of the Lead and the gaps between the test specimens in the experimental rods are accounted for. Also, the temperature levels anticipated in the test specimens are relevant for future practical applications. The validity of using average heat transfer correlations for the water cooled surfaces was demonstrated by a sample calculation using coupled fluid-structure analysis in one case.

1 Introduction

Since December 1996 the continuous spallation neutron source SINQ has been producing neutrons at Paul Scherrer Institute. The first target which is designed for a beam power of 1 MW, was made up of Zircaloy rods and is cooled by heavy water. In order to investigate radiation damage and thermomechanical behaviour of materials under irradiation in a realistic spallation environment, test rods will be put into SINQ-Target Mark 2 [4]. Among them are ten test sample rods containing more than 1500 specimens from different materials enclosed in Zircaloy-2 (Zy) tubes. Furthermore, some test elements relevant for the intended lead filled target (Mark 3) will be induced, as well as four solid steel rods. The test elements are 10.75mm diameter steel tubes, with 0.875mm wall thickness and filled with lead.

The temperature field and resulting mechanical load in the irradiated material is governed by the amount of heat deposited by the proton beam [6]. The thermal stress must be kept at reasonably low level to avoid surface and subsurface cracking of the material and hence a degradation of its performance. A thermal hydraulic analysis with conductive and convective heat transfer and a coupled structure mechanic examination is therefore indispensable.

The present paper describes the temperature and thermal stress analysis on the test rods, including heat transfer coefficient as well as the fluid velocity field through the rod bundle under conditions of a spallation environment. The calculations have been carried out by using the ANSYS-code with finite element method [2]. Special features such as material non-linearity, like plasticity, and contact resistance, have been taken into account.

Keywords: Rod target, Thermal stress, Lead plasticity, Heat transfer, Target cladding

2. Modelling for Coupled Heat Transfer and Thermomechanical Analyses

Fig. 1 shows part of the rod bundle arrangement in the experimental SINQ target. The test rods will be placed along the central axis of the target so that they will be exposed to different proton energies and intensities. According to the calculations by A. Dementyev et. al. [6], most energy will be deposited on the rods at the front of the target where the proton beam enters. So these rods will be examined first. Candidate tube materials for the lead filled rods are stainless steel HT-9, AlMgSi and Zircaloy.

The model used for the calculation is schematically shown in Fig.2. Energy conservation is applied for the steady state thermal conduction and convection calculation. Inside the rod (Fig. 2), the heat transfer process is governed by conduction, so that Fourier's law was used to relate the heat flux vector to the thermal gradient. The deposited power density q was taken from ref. [6] and was used here as an input parameter. On the rod surface, convective cooling by water prevails over the whole surface (with a water temperature T_b=50°C* and a velocity of 0.5m/s of the incoming flow). Therefore Newton's law of cooling was applied to determine the unknown surface temperature T_s.

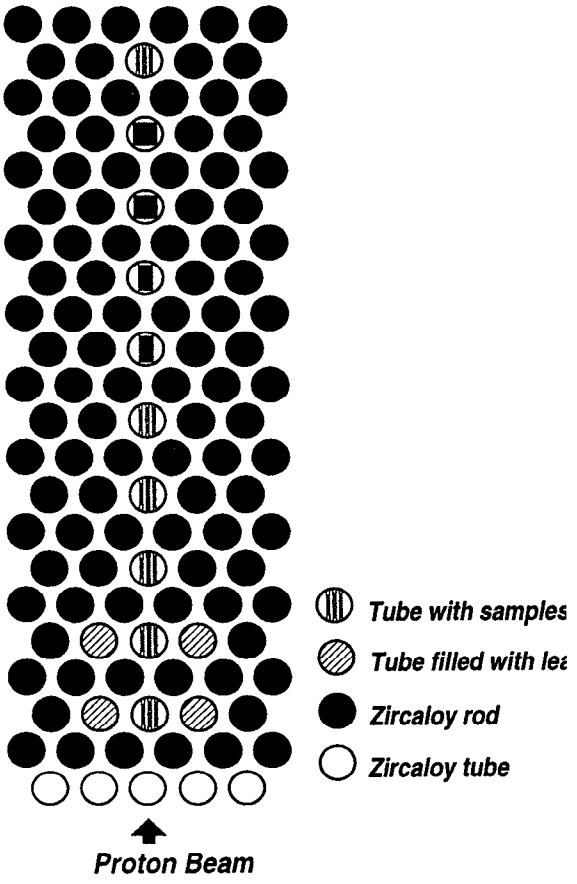

Fig. 1: *Arrangement of test rods in the SINQ Mark 2 (after [4])*

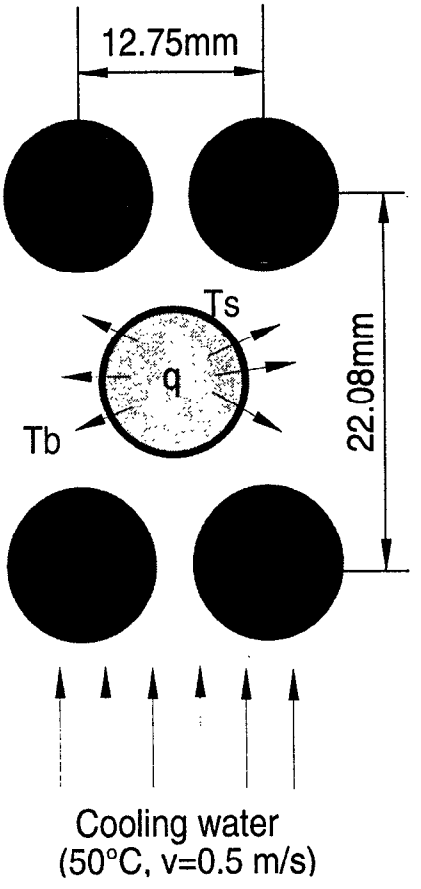

Fig. 2: *Computational model for heat transfer analysis*

* actually 40°C ;10°C safety margin

The average value of the wall heat transfer coefficient is determined from Nusselt and Reynolds number correlations for the staggered rod bundle according to [9]. For detailed studies it is, however, necessary to take into account that the wall heat transfer coefficient changes along the rod surface because of different local flow situations. This can be done by a fluid flow calculation. An example will be discussed in Section 5.

Having obtained the temperature field and the heat flux distribution, a steady state structure analysis could be applied to give detailed information on thermal stresses and deformations. A coupled thermal-structure analysis (Fig. 3) was performed in ANSYS, in which the coupling effects of the structural deformation on the thermal expansion are accounted for. The structural deformation may be plastic, such as in case of lead. Also the heat conduction resistance may have to be considered when the materials are not in perfect contact. Examples are treated in Section 4.

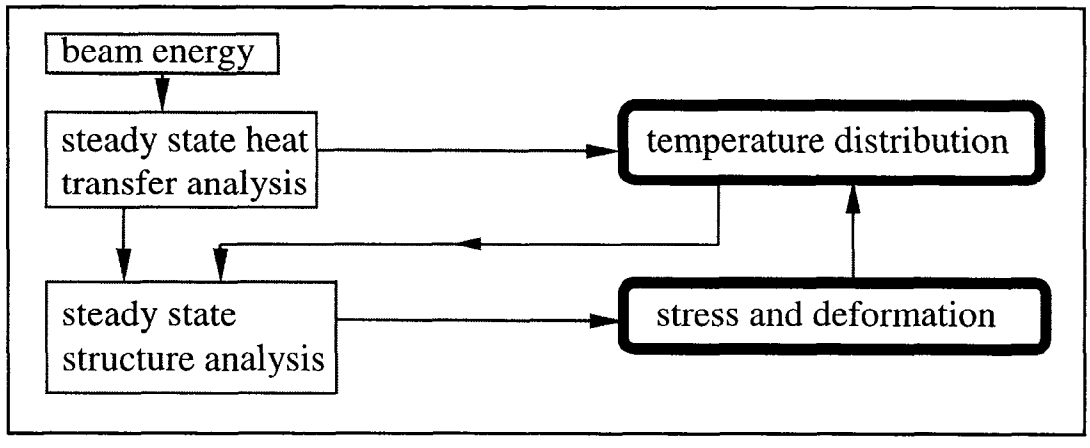

Fig. 3: *Coupled heat transfer and thermomechanic analysis procedure in ANSYS*

3. Thermomechanics of the Lead Filled Test Rods with and without Plasticity

Figure 4 shows the geometry of the test element. The possible maximum power density distribution along the length has been taken from the calculation by A. Dementyev et. al. [6] and is plotted in Fig. 5. The energy deposition over the rod cross-section was considered as uniform, because actual variations are small.

Since lead is quite a soft material, the stress-strain relation is very plastic, especially at high temperatures. Measured stress-strain curves for lead at 4 different temperatures, 22°C, 50°C, 99°C and 150°C, are given in ref [7] (Fig. 6). A plastic module was used in ANSYS, so that plasticity becomes active (i.e., plastic straining occurs) when the stress in the material exceeds its yield stress. Because of the symmetric geometry and power density distribution, only a quasi three-dimensional model was applied.

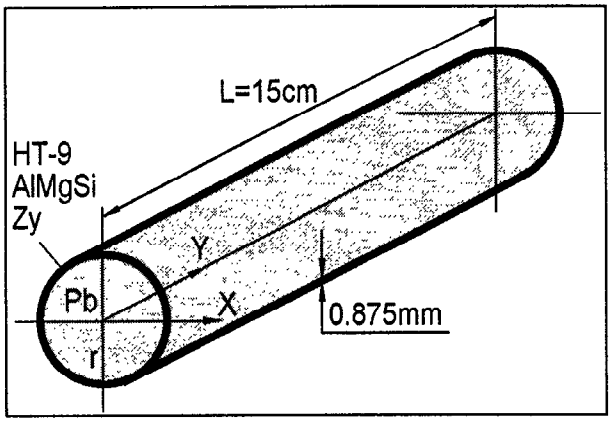

Fig. 4: *Geometry of the test rod*

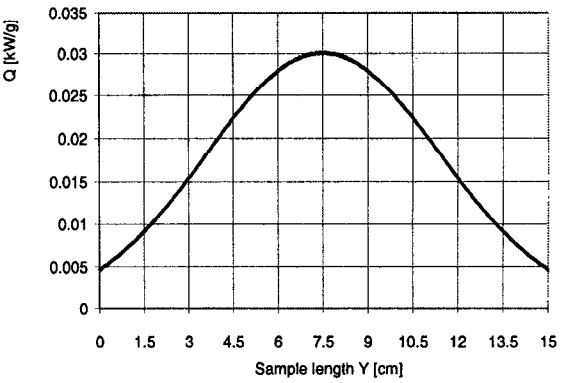

Fig. 5: *Power density distribution along the length of a lead filled rod*

In order to create a case for comparison the plasticity of lead was not taken into account in a first run. Figure "r98.ps46a" shows temperature and stress results on the HT-9 tube filled with lead, in which lead is assumed to be elastic only and both ends of the sample are free. In this picture, window "1" depicts the temperature distribution (TEMP in [°C]) in the rod, and window "2" the "equivalent" von Mises stress (designated as SEQV in [N/m^2]).The scale in horizontal direction, x, is five-fold enlarged to show the details. A maximum temperature of 167°C is found in the rod centre, where the highest energy deposition exists. The maximum von Mises stress of 377 MP appears in the middle part of the steel tube. DMX stands for the maximum total displacement (0.125mm) in the selected co-ordinate system (shown in the figure). Its main contribution comes from the axial component.

When the temperature dependent elastic-plastic stress-strain relations of the lead are taken into account, which is more realistic, the thermal stress decreases considerably due to plastic deformation. This case is presented in Figure "r98.ps46", where the maximum von Mises stress is now only 187 MP while the maximum total displacement, which now occurs at the free end, is increased to 0.557mm.

Results of the calculations for all three tube materials are listed in Table 1. As a general feature, the maximum temperature T_{max} occurs in the rod center, while the maximum von Mises stress $\sigma_{Mis,max}$ and the maximum hoop stress $\sigma_{\theta,max}$ (which is the important quantity for the safety of the target design) are found in the middle section of the tubes. It can be seen that, both HT-9 and Zy cladding result in relatively high temperature levels, while the moderately high stress occurs in the Zy tube. The rod with AlMgSi tube shows the lowest temperature level since AlMgSi has a much better thermal conductivity than the other two materials. With allowance made for plasticity of lead (the case with elastic behaviour only is not relevant in practice), the highest hoop stress is still found for HT-9 but is well below the design limit for this material. It should also be noted that, even when allowing plastic deformation of lead, perfect mechanical contact between the two metals is assumed and no slipping is allowed, which would further reduce the stress. The lowest rod surface temperature $T_{s,min}$ and the maximum total displacement U_{max} are also given in Table 1 for reference.

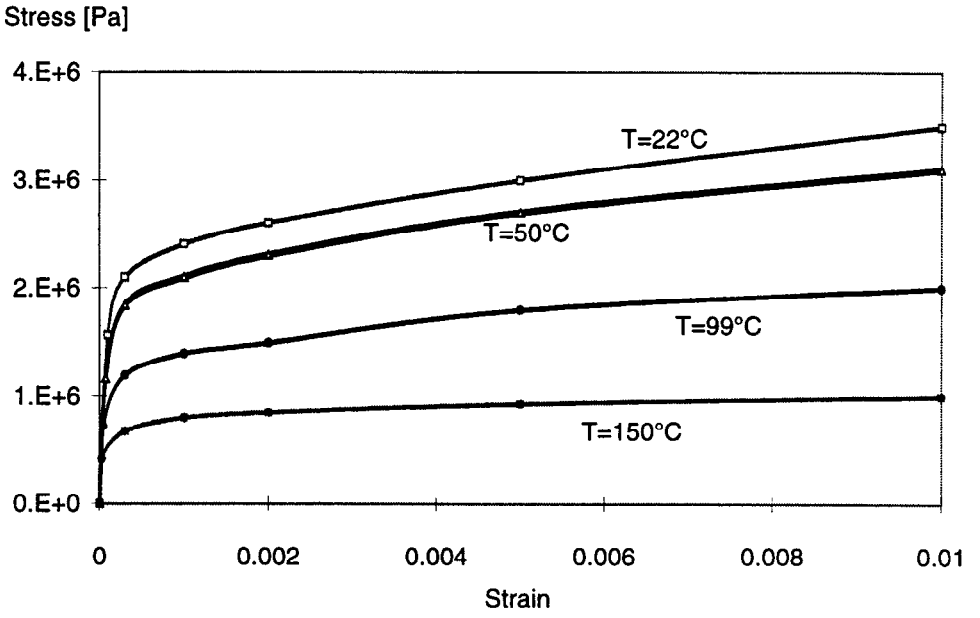

Fig. 6: *Stress-strain relations for lead (after [7])*

The role of the plasticity of lead can also be seen for the case shown in Fig. "r98.ps41b", where the HT-9 tube is not completely filled, leaving a gap of 1.1mm before heating. Because the temperature level (window "1") is highest at the free surface, the deformation shown in window "2" is mainly plastic (USUM stands for total displacement). The gap has narrowed by 0.0819mm. Without allowance of the plasticity the maximum displacement is only 0.0357mm and the stresses are much higher.

Table 1: *Thermomechanics results for test samples filled with lead*

Rod Design	Allowance for plasticity of lead	T_{max} [°C]	$T_{s,min}$ [°C]	$\sigma_{Mis,max}$ [MPa]	$\sigma_{\theta,max}$ [MPa]	U_{max} [mm]
HT-9 tube filled with Pb	no	167.32	59.25	377.	432.	0.125
HT-9 tube filled with Pb	yes	167.17	59.57	187.	215.	0.557
Al tube filled with Pb	no	144.09	59.78	61.9	68.8	0.151
Al tube filled with Pb	yes	144.10	59.78	60.8	70.6	0.136
Zy tube filled with Pb	no	170.23	59.26	237.	269.	0.12
Zy tube filled with Pb	yes	170.14	59.5	157.	185.	0.421

4. Experimental Rod with Perfect and Imperfect Internal Contact

In practice it is impossible to assemble a structure as complicated as our experimental rods without leaving any gaps inside. It is therefore important to examine the effect of such gaps on the temperature and stress levels in the specimens. For the time being only the middle cross-section of the rods where the highest energy deposition occurs has been examined for the ten experimental rods with test samples. A plane strain module was used to show the maximum possible stress. The input power density q [W/m^3] for the specimens inside the rod was again taken from Dementyev et. al. [6]. It is uniform for the same material but the value depends strongly on the heated material and on the position of the rod. We only present results here for the most heated -and hence most critical- rod. In particular we also examine the case where the specimens are imperfect in thermal contact among each other and with the fillers, i.e. interfacial gaps exist between two mating surfaces.

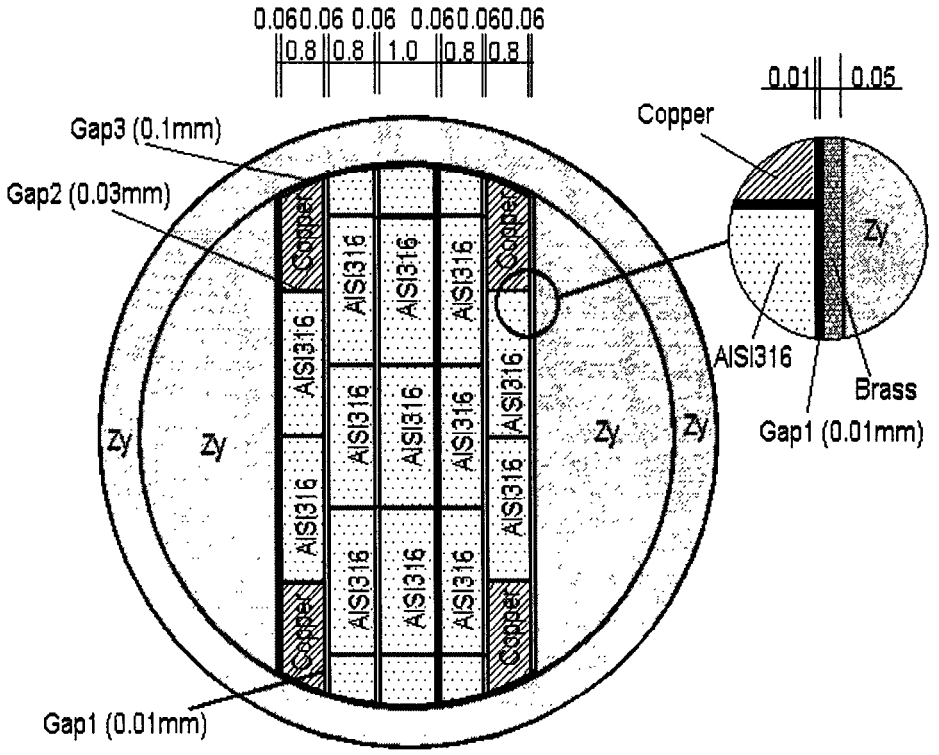

Fig. 7: *Cross-section of the rod with several layers of test specimens*

In Figure 7 the cross-section and the gap distribution of the test sample are displayed schematically. Boundary and water cooling conditions are the same as in Section 3. One quadrant of the cross-section was modelled only, because of symmetry. First the case with perfect contact (i.e. without gaps) was calculated. Figure "r98.ps37" shows distribution of the temperature (TEMP in window "1"), the total displacement (USUM in window "2"), the hoop stress σ_θ (SY in window"3") and the out-of-plane stress σ_z (SZ in window "4"). As can be seen, the maximum temperature T_{max} occurs in the rod centre. Although the maximum out-of-plane stress $\sigma_{z,min}$ runs

high (412MP), it occurs in the innermost material (AISI316) and is of no concern because it is compressive. In this case, both the maximum tensile hoop stress $\sigma_{\theta,max}$ (155MP) and the total displacement U_{max} appear at the top part of the Zy-tube. The maximum values for this case (designated as Nr. 1) are listed in Table 2 in order to compare with the cases of imperfect thermal contact.

Although the thermal stress values are clearly under the irradiation stress limit, it should be noted that this is for a hypothetical gap-free case. In practice such a situation cannot prevail, since it is impossible to mount the tiny specimens in an exact fit because of the manufacturing tolerance. Therefore, thermal contact resistance to heat flow exists between two mating surfaces. This resistance manifests itself in a sudden temperature drop at the interface which must not be ignored.

Thermal contact resistance depends not only on the material properties (such as hardness and conductivity), contact pressure and surface roughnesses, but also mainly on the sizes of interfacial gaps which are usually filled with gas [8]. In our case, the surface irregularities due to machining imperfections can be quite large, so that significant temperature jumps at the interfaces must be anticipated.

In our analysis with interface contact resistance, we assumed an equivalent gap thickness which is constant over the whole contact surface and Helium or air to be present in the interfacial gaps. Conduction in the gas phase was assumed as the dominant mode of heat transfer across the gaps. Observations [8] showed that convective heat transfer can be considered as negligible for gap widths up to a few millimetres. Also radiation was neglected because the temperatures at the both sides of the gaps are not very different. Besides, since the thermal conductivity of a gas is independent of its pressure [1], the conductance of a gas gap is insensitive to decreases in gas pressure until a certain "threshold pressure" is reached when the mean free path of the gas molecules λ becomes comparable in magnitude to the average gap width, which is beyond our consideration for the time being (for Helium: λ = 0.186μm and for air: λ = 0.064μm at atmospheric pressure). Under these circumstances, Fourier's law of heat conduction still applies to the gas layer which can then be treated as a continuum.

In Figure "r98.ps15", the temperature and the von Mises stress for the standard case (No. 3) with Helium in the gaps are plotted in window "1" and window "2", respectively. The maximum temperature in the rod centre rises from 166.7°C (without gap) to 258°C (with the most realistic gap widths: Gap1:Gap2:Gap3 = 10μm : 30μm : 100μm, cf. Fig 7). This temperature rise and the existence of contact resistance result in a higher stress level up to 641MP, which is (once again) compressive and occurs at the rod centre. The maximum hoop stress on the Zy-tube, $\sigma_{\theta,max}$=63.1 MP, is of no concern with respect to the stress design limit.

The temperature distribution along the horizontal radial direction without gaps and with He or air gaps is plotted in Fig. 8. The maximum temperature in the rod with air gaps (case No. 2) rises to almost 600°C because of the low thermal conductivity of air! This results in a very high stress level ($\sigma_{Mis,max}$ = 1690MP, cf. Table 2) which exceeds the allowable limit. From the point of view of heat transfer and cooling, Helium in the gaps is clearly to be preferred to air.

Table 2 lists the results of all calculations for this sample rod with different gap widths. In all cases, the temperature level increases due to gaps and the maximum temperature T_{max} occurs in the rod centre. The maximum von Mises stress $\sigma_{Mis,max}$ as well as the minimum out-of-plane stress $\sigma_{z,min}$ (which is compressive and contributes the main component to $\sigma_{Mis,max}$) also appear in the rod centre. It can also be seen that the rod is very sensitive to the width of "Gap1", since changing it from 5μm (case No. 4) to 20μm (case No. 5), has a strong effect on the temperature jump and therefore on the stress levels. By comparison, changing the width of "Gap 2" (from 10μm in case No. 6 to 50μm in case No. 7) and "Gap3" (from 20μm in case No. 8 to 200μm in case No. 9) makes no big difference on the temperature and stress levels. So we can conclude that it is very important to keep the width of "Gap1" as small as possible.

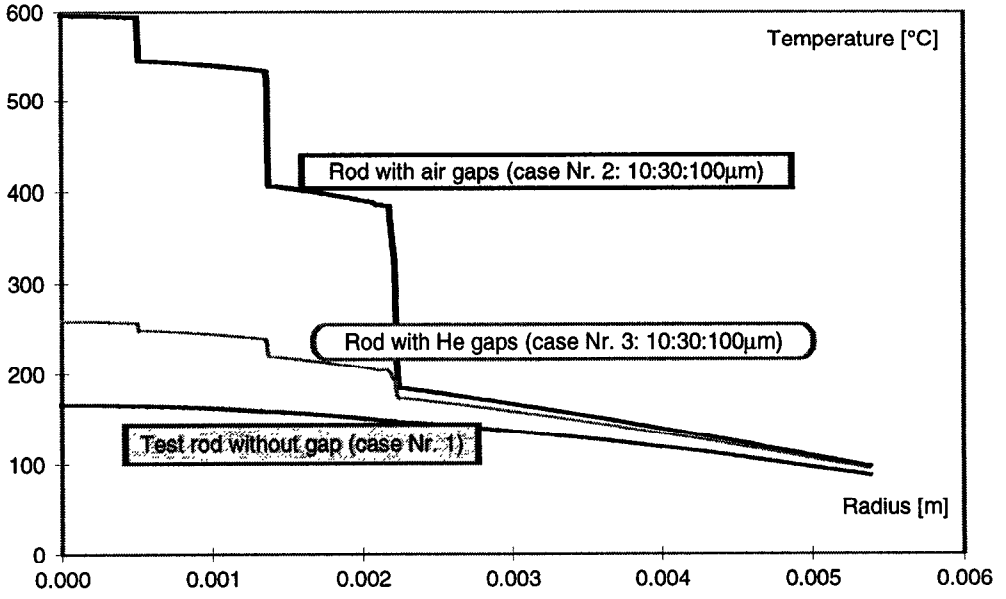

Fig. 8: *Temperature jumps in radial direction with and without gap*

It should be noted that the existence of the gaps affects the temperature and stress levels inside the test specimens but does not pose a risk to the integrity of the surrounding Zircaloy tube. The maximum tensile hoop stress on the Zy-tube $\sigma_{\theta,max}$ (not the maximum value inside the rod) which is also listed in Table 2 is found to decrease upon introduction of the gaps relative to case No. 1 ($\sigma_{\theta,max}$ =155MP). This is because "Gap3" allows the heated specimens inside the rod to expand freely and therefore the induced hoop stress on the tube becomes lower. The maximum total displacement occurs at the rod top (and bottom) where the largest gap width ("Gap3") was assumed. Even for case No. 2 which corresponds to an air filled gap of 100μm before heating, where U_{max} is found to be 56.5μm, the gaps have narrowed but are still not closed, which would improve the heat transfer, of course.

Table 2: *Results for the sample rod with perfect and imperfect interface contact*

Case number	No. 1	No. 2	No. 3	No. 4	No. 5	No. 6	No. 7	No. 8	No. 9
$q_{AISI316}$ [W/m^3]	2.7e8	2.7e8	2.7e8	2.7e8	2.7e8	2.7e8	2.7e8	2.7e8	2.7e8
q_{Zy} [W/m^3]	2.c8	2.e8	2.e8	2.e8	2.e8	2.e8	2.e8	2.e8	2.e8
q_{Brass} [W/m^3]	2.7e8	2.7e8	2.7e8	2.7e8	2.7e8	2.7e8	2.7e8	2.7e8	2.7e8
q_{Copper} [W/m^3]	2.7e8	2.7e8	2.7e8	2.7e8	2.7e8	2.7e8	2.7e8	2.7e8	2.7e8
Gap filling	no gap	Air	He	He	He	He	He	He	He
Gap1 [μm]	0.	10.	10.	5.	20.	10.	10.	10.	10.
Gap2 [μm]	0.	30.	30.	30.	30.	10.	50.	30.	30.
Gap3 [μm]	0.	100.	100	100.	100.	100.	100.	20.	200.
T_{max} [°C]	166.69	596.17	258.01	228.08	313.24	257.65	257.88	230.83	267.63
$T_{s,min}$ [°C]	87.6	70.47	74.34	73.02	76.61	74.51	74.2	85.99	70.25
$\sigma_{Mis,max}$ [MP]	323.	1690.	641.	549.	812.	640.	641.	558.	671.
$\sigma_{\theta,max}$ [MP]	155.	61.7	63.1	58.8	59.4	46.9	51.5	51.9	56.5
$\sigma_{z,min}$ [MP]	-412.	-1690.	-643.	-551.	-814.	-642.	-643.	-559.	-673.
U_{max} [μm]	7.82	56.5	20.9	17.8	26.6	20.8	20.9	15.9	30.6

5 Simulation of the Coolant Flow through the Heated Rod Bundle

While the foregoing calculations were made under the assumption of a constant heat transfer coefficient along the rod surface, the actual local wall heat transfer coefficient depends on the flow pattern around the rod surface. In order to estimate this effect, the flow field around the rods and the local heat transfer were modelled by using the ANSYS submodule FLOTRAN. At the same time, the heat transfer within the rod and the corresponding stress distribution were investigated by means of a coupled ANSYS/ FLOTRAN and ANSYS/MULTIPHSICS analysis. Details of this analysis will be reported elsewhere. Here we only show the main features and the first results of the coupled thermal hydraulic and thermomechanic approach by ways of an example.

Lines in Fig. "r98.p72" show the modelled section of the rod bundle including fluid and non-fluid (solid rods) regions . The incoming flow from bottom was assumed to be uniform (with a velocity of 0.5m/s at a temperature of 50°C) and the exit pressure was set to zero. Periodic boundary conditions were applied on both right and left boundary lines. In the solid rods, the case of lead filled, 0.875mm thick Zy-tubes was considered, and an uniform power density with a maximum value of 280 W/cm^3 was used. Contrary to Section 3, the convective heat transfer around the rod surface is now considered as a function of position.

Figure "r98.p72" gives the velocity and pressure distributions of the flow field around the rods. There is very little temperature rise in the fluid. The left picture of Fig. "r98.p75" (window "1") displays the temperature field in the left half of the central rod. As can be seen, the maximum temperature in the central rod changes marginally to 169°C, (as compared to 167°C in the uniform cooling case, Fig. "r98.ps46"), and it is slightly asymmetric between the upstream (bottom half of the rod) and downstream (top half of the rod) side because of the different local flow status. Hot spots occur at both stagnation points where the temperature reaches a maximum value of 132°C. The difference between the highest and lowest temperature on the surface is 46K (Fig "r98.p75" and Fig. 9).The calculated flow-dependent heat transfer coefficient is shown in Fig. 9, in comparison to the average value obtained from an empirical relation in ref [9].

In order to examine the effect on the stress in the cladding we used the case of no plastic deformation in the lead since we were working in a plane stress model only. As noted before, this results in higher stress levels than expected in reality, but the effect of local variation should be roughly the same. The right picture in Fig. "r98.p75" depicts the von Mises stress in the central rod as calculated, accounting for the local variations of the heat transfer. The comparison with the corresponding results based on the average heat transfer coefficient in window "1" and window "2" of Fig. "r98.p76" shows that the maximum von Mises stress on the tube is slightly higher in the "local" case (319MP), than in "average" case (311MP). These results show that in the present situation the precision of predictions based on the average heat transfer are well within usual engineering safety margins. However, if the safety margin becomes small or the local properties, such as hot spots, are of special interest, a coupled fluid-structure analysis shall be used.

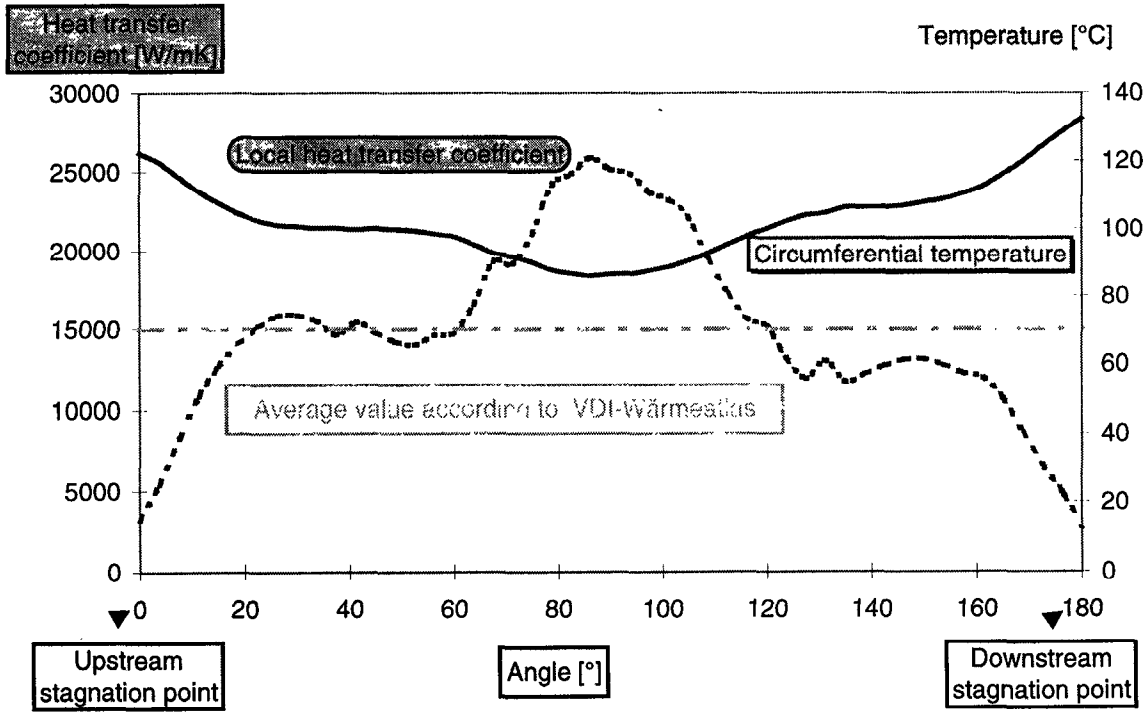

Fig. 9: *Local heat transfer coefficient and temperature distribution along the rod surface*

6. Conclusions

A sample calculation of the coupled fluid-structure analysis based on the local flow pattern, which is time-consuming, demonstrated that this procedure need only be applied if stress safety margins are very small or if the local properties such as hot spots are of special interest.

The coupled heat transfer and thermomechanic analysis, although carried out under the somewhat simplifying assumption of a constant heat transfer coefficient over the rod surface, showed that

- temperature and stress levels in the test samples of the SINQ target Mark 2 are in the range where they would also be anticipated in a real application of the tested materials;
- stress levels on the enclosure tubes (Zircaloy) are not a problem for this material;
- using Helium to fill the gap between test specimens and fillers will lead to significantly lower temperature levels in the specimens than having air in the gaps.
- for the lead filled HT-9 tubes moderate hoop stress levels can be expected if the plasticity of the lead is accounted for and the tubes are not completely filled;

While the cases with and without gap are clearly limiting cases not possible in the real specimen arrays because neighbouring layers will always touch at some points and develop a gap in other regions, it is comforting to see that all cases lead to stress levels within the safe range of application of the materials concerned, especially those used for the enclosure tubes.

References

[1] Aaron, R.L.: "A Theroretical Study of the Thermal Conductance of Joints with Varying Ambient Pressure" MS Thesis, Southern Methodist University, Dallas, 1963

[2] ANSYS Revision 5.3, 1997, Swanson Analysis Systems, Inc.

[3] Bauer, G.S. & Dai, Y., PSI Annual Report 1996/Annex IIIA, p.5.

[4] Bauer, G.S., Dai, Y. and Ni, L.: "Experience and Research on Target and Structural Materials at PSI", The International Workshop on JHF Science (JHF98), High Energy Accelerator Reasearch Organization (KEK), Tsukuba, Japan, March 4-7, 1998.

[5] Dai, Y., PSI Annual Report 1997/Annex IIIA

[6] Dementyev , G.S. Bauer Y. Dai and E. Lehmann: "Neutronic Aspects of the SINQ Mark 2 Target with Irradiation Test Samples" this conference

[7] Kalkhof, D & Kamber, J.: "Zugversuche an Bleiproben als Beitrag für die SINQ-Targetentwicklung", PSI-Dokumentation, TM-49-97-09

[8] Madhusudana, C.V.: "Thermal contact Conductance", Mechanical Engineering Series, New York (etc.), Springer, cop. 1996, ISBN 0-387-94534-2

[9] VDI-Wärmeatlas: "Berechnungsblätter für den Wärmeübergang", Springer-Verlag Berlin Heidelberg, 1997

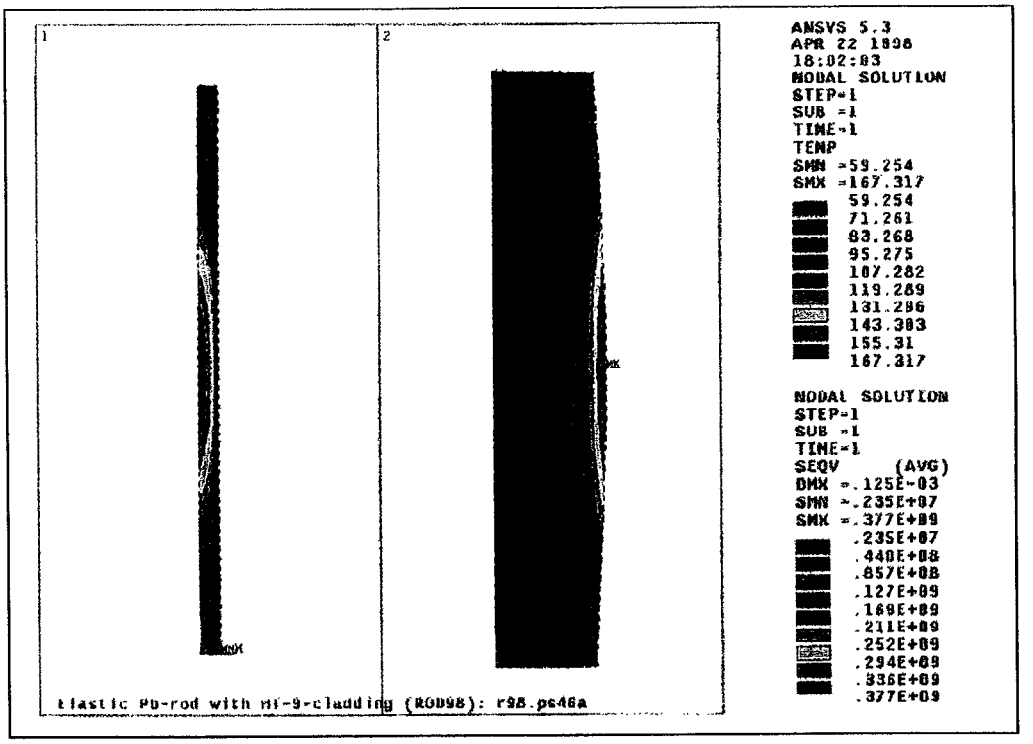
1
2
ANSYS 5.3
APR 22 1998
18:02:03
NODAL SOLUTION
STEP=1
SUB =1
TIME=1
TEMP
SMN =59.254
SMX =167.317
59.254
71.261
83.268
95.275
107.282
119.289
131.296
143.303
155.31
167.317
NODAL SOLUTION
STEP=1
SUB =1
TIME=1
SEQV (AVG)
DMX =.125E-03
SMN =.235E+07
SMX =.377E+08
.235E+07
.440E+07
.857E+07
.127E+08
.169E+08
.211E+08
.252E+08
.294E+08
.336E+08
.377E+08
Elastic Pb-rod with Hf-9-cladding (ROD98): r98.ps46a

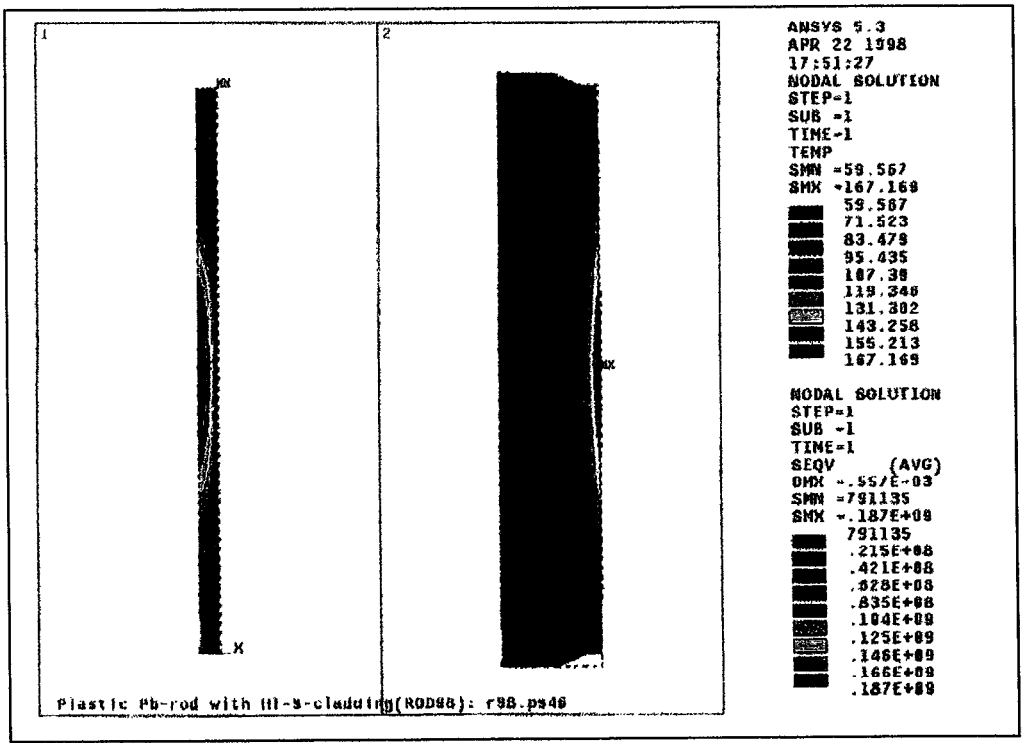
1
2
ANSYS 5.3
APR 22 1998
17:51:27
NODAL SOLUTION
STEP=1
SUB =1
TIME=1
TEMP
SMN =59.567
SMX =167.169
59.567
71.523
83.479
95.435
107.38
119.346
131.302
143.258
155.213
167.169
NODAL SOLUTION
STEP=1
SUB =1
TIME=1
SEQV (AVG)
DMX =.557E-03
SMN =791135
SMX =.187E+08
791135
.215E+07
.421E+07
.628E+07
.835E+07
.104E+08
.125E+08
.146E+08
.166E+08
.187E+08
Plastic Pb-rod with Hf-9-cladding(ROD98): r98.ps46

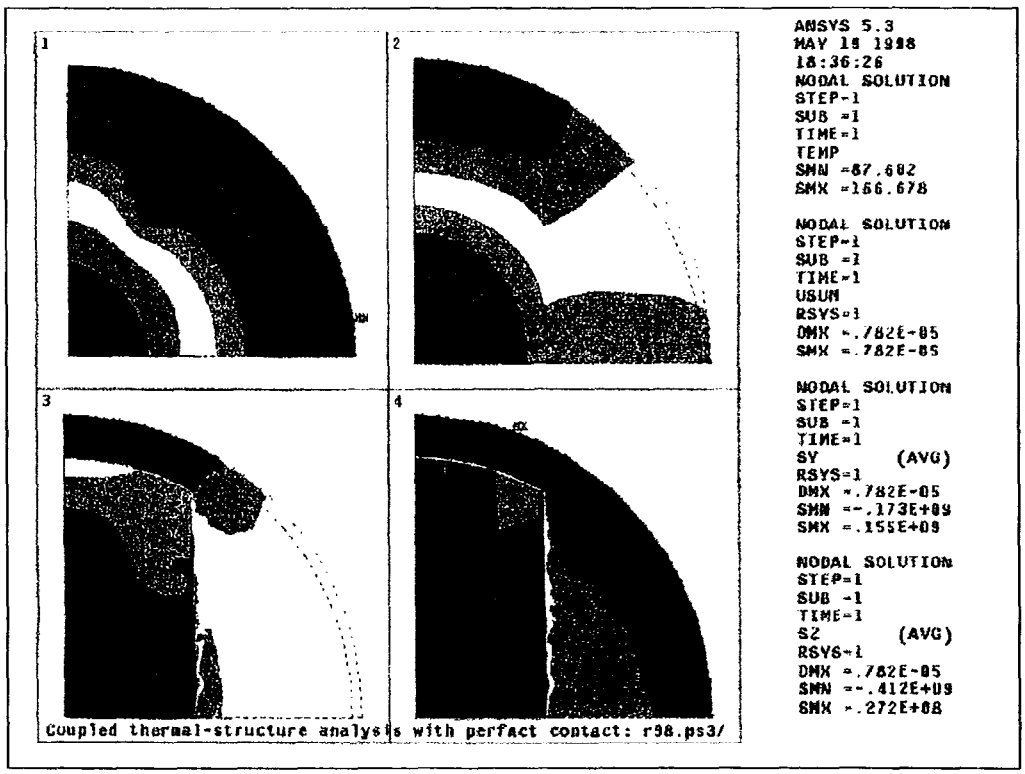
1
2
3
4
ANSYS 5.3
MAY 18 1998
18:36:26
NODAL SOLUTION
STEP=1
SUB =1
TIME=1
TEMP
SMN =87.682
SMX =166.678
NODAL SOLUTION
STEP=1
SUB =1
TIME=1
USUM
RSYS=1
DMX =.782E-05
SMX =.782E-05
NODAL SOLUTION
STEP=1
SUB =1
TIME=1
SY (AVG)
RSYS=1
DMX =.782E-05
SMN =-.173E+09
SMX =.155E+09
NODAL SOLUTION
STEP=1
SUB =1
TIME=1
SZ (AVG)
RSYS=1
DMX =.782E-05
SMN =-.412E+09
SMX =.272E+08
Coupled thermal-structure analysis with perfect contact: r98.ps3/

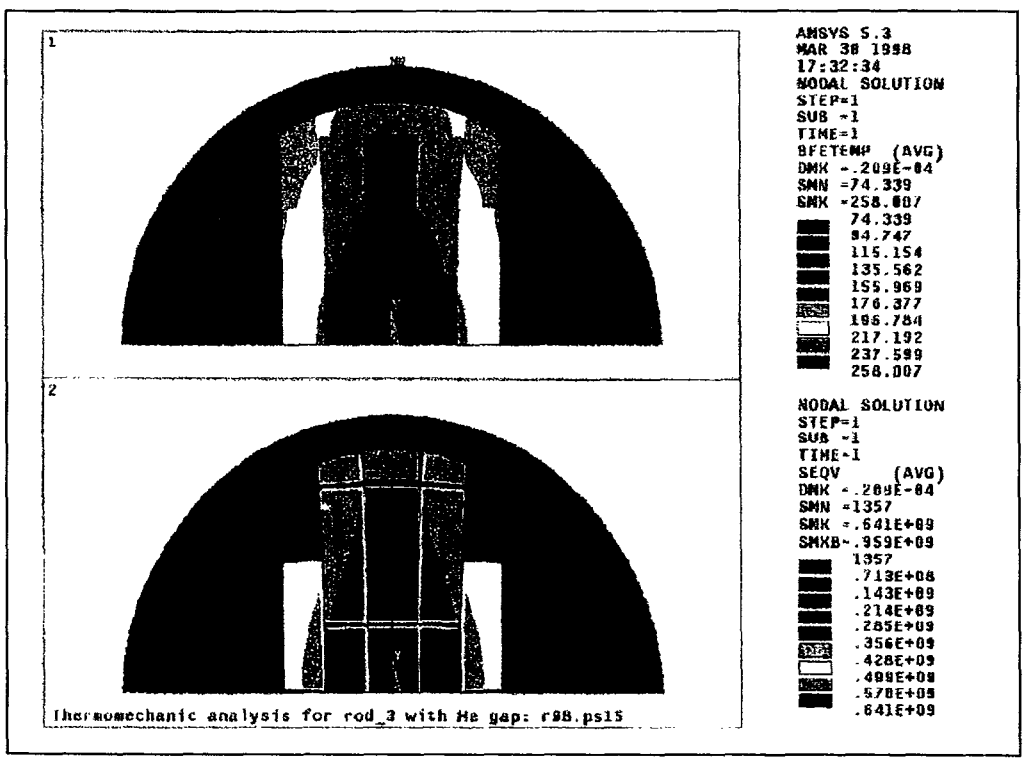
1
2
ANSYS 5.3
MAR 30 1998
17:32:34
NODAL SOLUTION
STEP=1
SUB =1
TIME=1
BFETEMP (AVG)
DMX =.209E-04
SMN =74.339
SMX =258.007
74.339
94.747
115.154
135.562
155.969
176.377
196.784
217.192
237.599
258.007
NODAL SOLUTION
STEP=1
SUB =1
TIME=1
SEQV (AVG)
DMX =.209E-04
SMN =1357
SMX =.641E+09
SMXB=.959E+09
1357
.713E+08
.143E+09
.214E+09
.285E+09
.356E+09
.428E+09
.499E+09
.570E+09
.641E+09
Thermomechanic analysis for rod_3 with He gap: r98.ps15

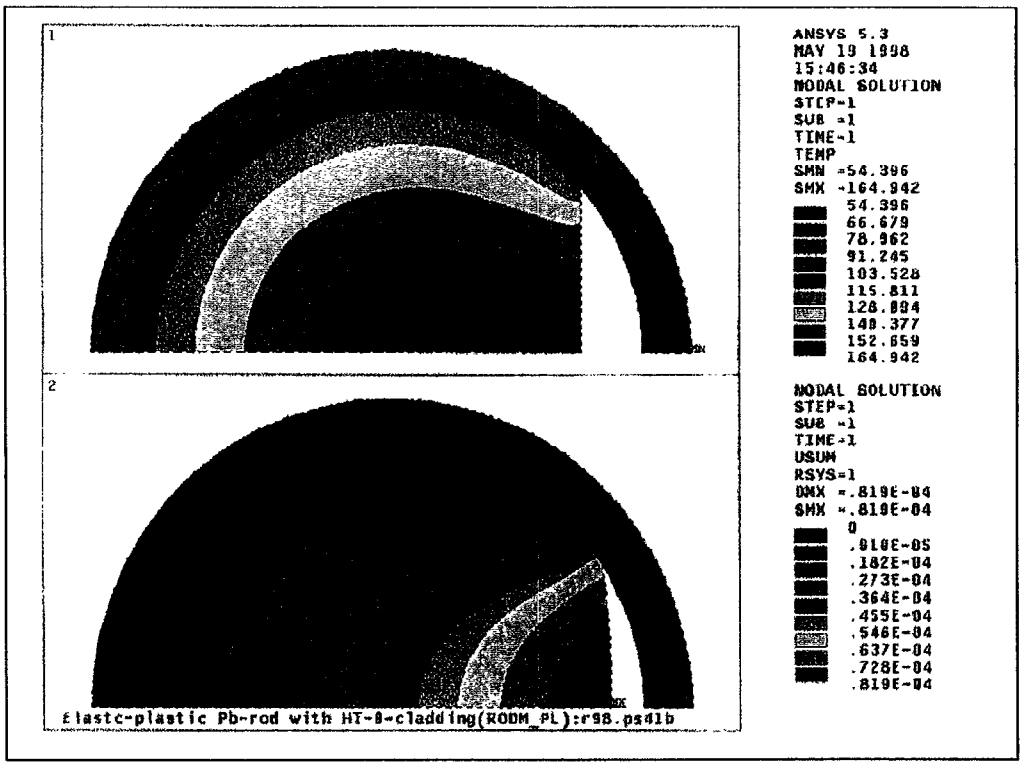
1
2
ANSYS 5.3
MAY 19 1998
15:46:34
NODAL SOLUTION
STEP=1
SUB =1
TIME=1
TEMP
SMN =54.396
SMX =164.942
54.396
66.679
78.962
91.245
103.528
115.811
128.094
140.377
152.659
164.942
NODAL SOLUTION
STEP=1
SUB =1
TIME=1
USUM
RSYS=1
DMX =.819E-04
SMX =.819E-04
0
.910E-05
.182E-04
.273E-04
.364E-04
.455E-04
.546E-04
.637E-04
.728E-04
.819E-04
Elastc-plastic Pb-rod with HT-9-cladding(RODM_PL):r98.ps41b

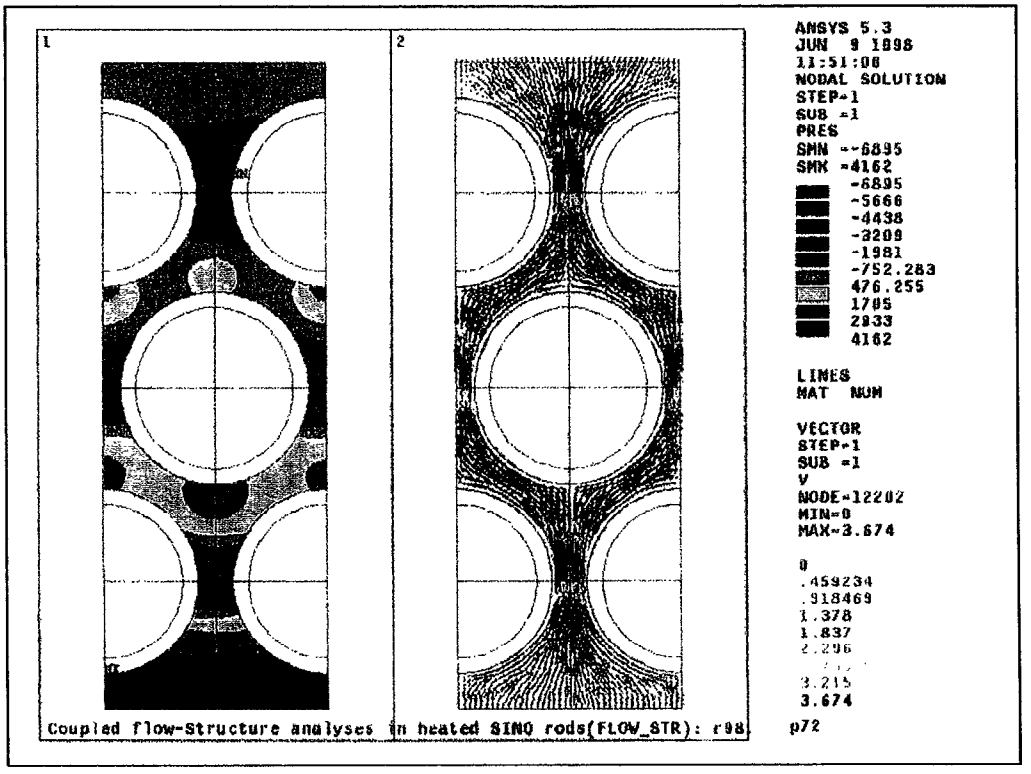
1
2
ANSYS 5.3
JUN 9 1998
11:51:08
NODAL SOLUTION
STEP=1
SUB =1
PRES
SMN =-6895
SMX =4162
-6895
-5666
-4438
-3209
-1981
-752.283
476.255
1705
2933
4162
LINES
MAT NUM
VECTOR
STEP=1
SUB =1
V
NODE=12202
MIN=0
MAX=3.674
0
.459234
.918469
1.378
1.837
2.296
3.215
3.674
Coupled flow-Structure analyses in heated SINQ rods(FLOW_STR): r98
p72

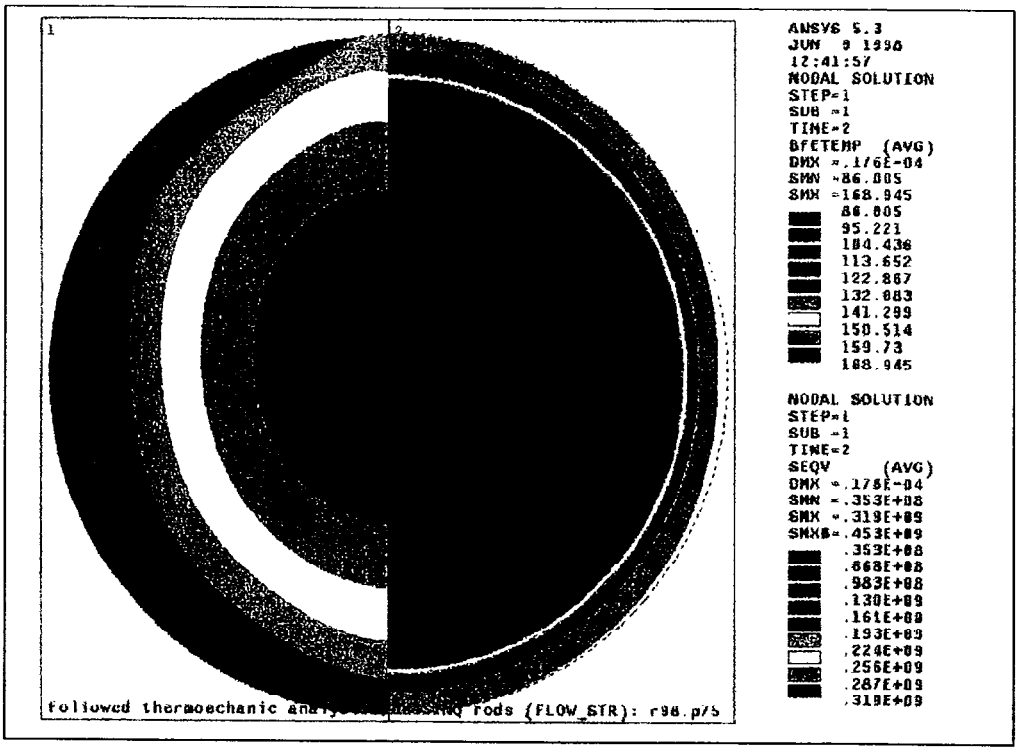
1
2
ANSYS 5.3
JUN 9 1998
12:41:57
NODAL SOLUTION
STEP=1
SUB =1
TIME=2
BFETEMP (AVG)
DMX =.176E-04
SMN =86.805
SMX =168.945
86.805
95.221
104.436
113.652
122.867
132.083
141.299
150.514
159.73
168.945
NODAL SOLUTION
STEP=1
SUB =1
TIME=2
SEQV (AVG)
DMX =.178E-04
SMN =.353E+08
SMX =.319E+09
SMX=.453E+09
.353E+08
.668E+08
.983E+08
.130E+09
.161E+09
.193E+09
.224E+09
.256E+09
.287E+09
.319E+09
followed thermoechanic ana
rods (FLOW_STR): r98.p75

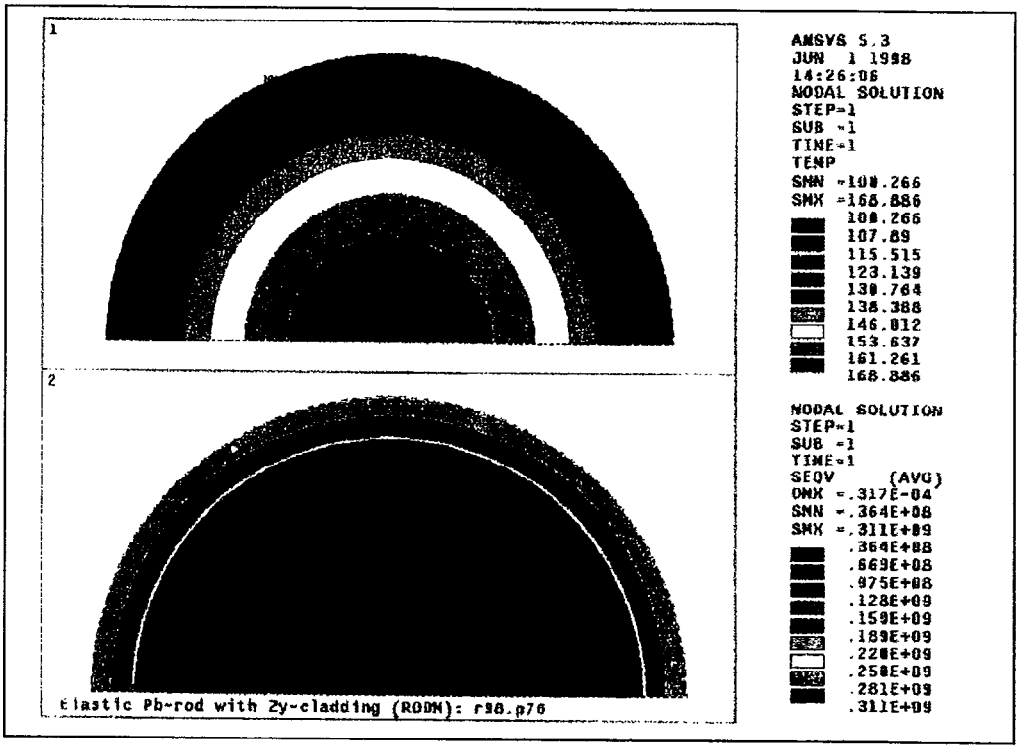
1
2
ANSYS 5.3
JUN 1 1998
14:26:06
NODAL SOLUTION
STEP=1
SUB =1
TIME=1
TEMP
SMN =100.266
SMX =168.886
100.266
107.69
115.515
123.139
130.764
138.388
146.012
153.637
161.261
168.886
NODAL SOLUTION
STEP=1
SUB =1
TIME=1
SEQV (AVG)
DMX =.317E-04
SMN =.364E+08
SMX =.311E+09
.364E+08
.669E+08
.975E+08
.128E+09
.159E+09
.189E+09
.220E+09
.250E+09
.281E+09
.311E+09
elastic Pb-rod with Zy-cladding (RODN): r98.p76